analytical chemistry

Article

Cite This: Anal. Chem. 2019, 91, 15235−15239

pubs.acs.org/ac

Discovery of Small-Molecule Sulfonamide Fluorescent Probes for GPR120

Pan Liu,[#] Siyue Ma,[#] Chongzheng Yan, Xiaojun Qin, Pei Zhao, Qi Li, Yuanyuan Cui, Minyong Li, and Lupei Du*

Department of Medicinal Chemistry, Key Laboratory of Chemical Biology (MOE), School of Pharmacy, Shandong University, Jinan, Shandong 250012, China

Supporting Information

ABSTRACT: GPR120 is a novel target for the treatment of metabolic disease and type 2 diabetes. The small-molecule fluorescent probe could help us locate GPR120 visually and guide in-depth study of GPR120. In this study, we synthesized six nonacidic sulfonamide fluorescent probes and tested their optical and biological properties. Compared to previous probes for GPR120, these probes, with sulfonamide structure, have high selectivity on GPR120. We used these probes to establish a BRET binding assay system to screen agonists and antagonists of GPR120. It is expected that these novel fluorescent probes may become useful tools in studying pharmacology and physiology of GPR120.

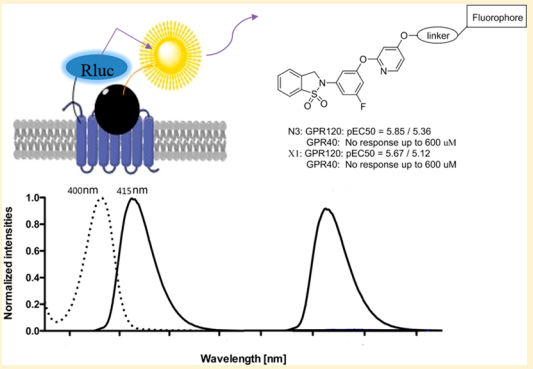

GPR120 [G protein-coupled receptor 120, also known as free fatty acid receptor 4 (FFA4), which is targeted by long-chain fatty acids,[1] was first found to be a potential antidiabetic target in 2005 to treat type 2 diabetes mellitus.[2] At the tissue level, GPR120 is expressed mainly in the liver,[3] lung,[2] intestine,[4] and adipose tissue.[3] However, at the cellular level, GPR120 is mainly distributed in macrophages, taste cells, enteroendocrine cells, and adipose cells.[2,5] A previous study showed that the activation of GPR120 could promote the secretion of insulin,[6] regulate hormone secretion in the pancreas and gastrointestinal tract, adjust lipid and glucose metabolism in adipose tissue,[7] reduce inflammation in macrophages, and induce the secretion of cholecystokinin (CCK) and glucagon-like peptide-1 (GLP-1) in the endothelium cells of the intestine.[2,8−10]

So far, carboxylic probes[11] were found to be intrinsically active on G protein-coupled receptor 40 (GPR40) because the pharmacophore was similar to that of free fatty acids.[1,12] To study the mechanism of GPR120 in more depth and conduct drug screens more easily, we aimed to synthesize small-molecule fluorescent probes tracing GPR120 with high selectivity for GPR120. First, we searched for novel structures as the pharmacophore. Compounds that bind to GPR120 can be divided into two categories, carboxylic acids and sulfonamides, respectively. TUG-1197[13] and GSK137647A[14] are nonacidic sulfonamide GPR120 agonists. TUG-1197 showed a pEC_{50} of 6.91 ± 0.04 in the β-arrestin-2 assay and an EC_{50} of 234 nM in the Ca^{2+} assay on GPR120, which showed no activity at GPR40.[13] GSK137647A was evaluated to provide at least 100-fold selectivity on GPR120 against GPR40.[14] To date, TUG-1197 has been used in vivo in rodents to study insulin sensitivity and glucose metabolism. Because of poor solubility and uncertainty of the combination pocket, GSK137647A had not yet been used for in vivo experiments. Considering pharmacokinetic and pharmacodynamics properties, we choose to modify TUG-1197 as the pharmacophore.

Naphthalimides[15] and coumarin groups[16−18] were fluorophore groups. The fluorescence intensity of them varied greatly in different polar environments. Their reasonable fluorescent properties enabled them to serve as fluorophores to locate and trace GPR120 when probes bind to the hydrophobic site. Subsequently, two series of fluorescent agonists were synthesized and characterized (Scheme 1).

Once binding occurred to the key anchoring point of GPR120, the fluorescence intensity of probes increased significantly, allowing the probes to be conveniently applied to the localization, visualization, and real-time monitoring. Bioluminescence resonance energy transfer (BRET) was used to measure the binding affinity between GPCRs (G protein-coupled receptors) and compounds.[19] Because the values used are ratios, the BRET binding assay can avoid background effects. Therefore, we selected probes to establish a screening assay for GPR120 with the BRET assay, where DeepBlue C is the substrate.[20]

Received: September 12, 2019
Accepted: November 6, 2019
Published: November 6, 2019

DOI: 10.1021/acs.analchem.9b04157
Anal. Chem. 2019, 91, 15235−15239

Scheme 1. Design of Fluorescent Probes for GPR120

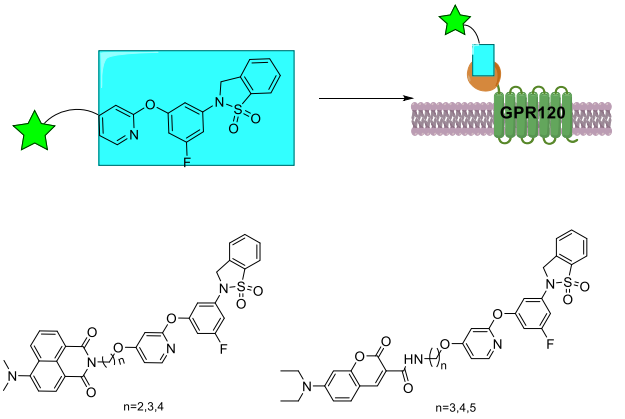

EXPERIMENTAL SECTION

Synthesis. The fluorescent probes **N1**−**N3** and **X1**−**X3** were synthesized (as shown in Scheme 1). The benzosultam intermediate **1**, obtained from saccharin, typically goes through Ullmann coupling to give intermediate **2**.[13] Another diaryl ether bond was formed by Ullmann reaction. **X1**−**X3** was obtained after reduction and ammonolysis. (More details can be found in Schemes S1−S4, Supporting Information.)

Optical Property Evaluation for Probes. Probes were completely dissolved in dimethyl sulfoxide (DMSO) as stock solution (40 mM). The stock solution was blended with phosphate buffered saline (PBS, pH 7.4). The fluorescence spectra and UV absorbance spectra were scanned in PBS (10 μM). Moreover, we confected solutions with different solvents including water, DMSO, methanol, acetonitrile, dichloromethane (10 μM), and solutions by concentration gradients of probes in PBS (pH 7.4). Their excitation and emission spectra were measured by an Edinburgh Instruments FLS920 spectrofluorometer.

BRET-Based β-Arrestin-2 Activity Assay.[21] HEK293 cells were encoded with plasmids GPR120-YFP and β-arrestin-2-Rluc. Cells were cultured at 37 °C for 24 h before use. After the cells were washed with Hank's Balanced Salt Solution (HBSS), 100 μL of coelenterazine (5 μM) and probes were added. After 2 min of Co-incubation, the fluorescence intensity of the solution at 460 and 520 nm was measured by a POLARstar Omega microplate reader.

Calcium Flux Activity Assay.[22] The expriment was conducted using HEK293 cells stably transfected by plasmids GPR120-Rluc. Cells were incubated in a 96-well black plate (2×10^4) for 24 h. After the medium was extracted from each well, Fluo3-AM (a calcium indicator) operating fluid (4 μM), was added (40 μL each well) and cultured in the incubator for 15 min. Different concentrations of compounds were prepared in HBSS and then were added into the plate (160 μL each well). The plate remained in the incubator for 20 min and was washed by (4-(2-hydroxyethyl)-1-piperazineethanesulfonic acid) (HEPES). After 200 μL of HEPES was added, the plate was read by a POLARstar Omega microplate reader at 530 nm (Ex 480 nm).

In another experiment, CHO cells encoded with plasmids GPR40 were cultured. The activity of compounds TAK875, L6, **N3**, and **X1** were measured. TAK875 was the agonist of GPR40.[23] L6 was the carboxylic probe of GPR120. The procedure was the same as that used above.

Cytotoxicity Assay. CCK-8 assay was used to obtain IC_{50} of probes cultured with HEK293 cells and PC-3 cells. Cells were added in 96-well plates (100 μL, 1×10^5 each well) and incubated for 24 h. One hundred microliters of concentration gradients of probes in medium (without FBS (fetal bovine serum)) was added into plates and the plates were incubated for another 24 h. Finally, the medium was replaced by CCK-8 working solution. After incubation for 1 h, the absorbance was measured by a POLARstar Omega microplate reader.

Fluorescence Imaging and Monitoring. HEK293 cells and PC-3 cells were cultured in a confocal dish (1 mL, 3×10^3) for 18 h. After the medium was poured into culture dishes, probes in medium without FBS were added (1 mL, 200 nM). After incubation for 10 min, the confocal dish was observed by an inversion fluorescence microscope. To monitor internalization of GPR120, we observed the confocal dishes (**N3** and **X1**) in real time.

Saturation BRET Binding Experiments. The cell membrane proteins of GPR120-Rluc stable transfected HEK293 cells were prepared. Membrane was preserved in Tris-HCl assay buffer (1 mM $MgCl_2$, 10 mM KCl, pH 7.4). The membrane was co-incubated with a different concentration of **N3** (or **X1**) for 40 min. After addition of DeepBlue C (1 μM) for 2 min, the plate was detected at 420 and 520 nm for **N3** (420 and 460 nm for **X1**). An excess amount of TUG-1197 (10 μM) was added in nonspecific binding groups.

Kinetic BRET Binding Experiment. In the kinetic BRET binding experiment, cell membrane was collected in the same manner as the equilibrium assay and was added to 96-well black plates with DeepBlue C. After co-incubation for 5 min at 37 °C, the BRET value was monitored by the microplate reader at 30 s intervals for 1 min. Association experiments were initiated by adding **N3** (or **X1**), 50 nM concentration. After the values were scanned at 30 s intervals for 5 min, dissociation experiments were conducted by adding TUG-1197 (5 μM). The reading was continued at 30 s intervals for 35 min.

Table 1. Spectroscopic Properties and Pharmacologic Properties

						GPR120[c]		IC_{50}[d] (μM)	
probe	λ_{abs} (nm)	λ_{ex} (nm)	λ_{em} (nm)	SS[a]	Φ[b]	β-Arr.pEC$_{50}$	Ca^{2+}.pEC$_{50}$	HEK293	PC-3
N1	448	415	530	115 nm	4.61%	5.25 ± 0.23	4.97 ± 0.27	52.0 ± 7.5	444 ± 4.6
N2	449	420	525	105 nm	3.00%	5.70 ± 0.16	5.15 ± 0.09	51.7 ± 4.8	169 ± 1.1
N3	449	415	530	115 nm	4.51%	5.85 ± 0.28	5.36 ± 0.09	313 ± 1.3	303 ± 3.1
X1	427	415	475	60 nm	7.54%	5.67 ± 0.28	5.12 ± 0.20	160 ± 1.2	226 ± 2.9
X2	434	410	470	60 nm	10.5%	5.22 ± 0.36	4.88 ± 0.23	514 ± 1.8	137 ± 2.9
X3	433	410	470	60 nm	9.18%	5.12 ± 0.28	4.76 ± 0.25	541 ± 1.3	198 ± 3.1

[a]SS, Stokes shift. [b]Φ, absolute quantum yield in PBS buffer. [c]Biological activity obtained by β-arrestin-2 activity assay and calcium flux activity assay. [d]IC_{50} value was obtained from CCK-8 assay.

DOI: 10.1021/acs.analchem.9b04157
Anal. Chem. 2019, 91, 15235−15239

Displacement BRET Binding Assays. Cell membrane was collected in the same manner as above. Test compounds were configured in different concentrations by assay buffer (10 mM KCl, 1 mM $MgCl_2$, 50 mM Tris-HCl, pH 7.4). A suspension composed of 50 nM probes, 0.15 mg/mL membrane, and test compounds was added to 96-well black plates (100 μL each well). After the plates were shaken in a thermostatic oscillator at 37 °C for 40 min, DeepBlue C was added to the plates (1 μM final concentration). After incubation for 5 min, fluorescence intensity was detected at 420 and 520 nm for **N3** (420 and 460 nm for **X1**).

RESULTS AND DISCUSSION

Optical Property Evaluation for Probes. The optical properties including fluorescence spectra, ultraviolet spectrum, and the relative quantum yield are shown in Table 1.

As predicted, the maximum UV absorption of these probes was in the range of 425−450 nm. Moreover, the fluorescent emission wavelength of **N1**−**N3** was in the green range at 525−530 nm, while **X1**−**X3** was in the blue range at 470−475 nm (details in Figure S1). The excitation wavelength of probes was in the range of 410−420 nm. The minimum Stokes shift in the biological system was 30 nm; if Stokes shift is less than 30 nm, the fluorescence excitation and emission spectrum will seriously interfere with each other. Because the Stokes shift of these probes was at least 60 nm, each probe can avoid the interference of the excitation light on the emitted light. To obtain the relative quantum yield, fluorescein sodium was used as a control group. The relative quantum yield of probes was observed at about 5%.

By measuring the fluorescence spectra of compounds at different concentrations, we found the fluorescence intensity of probes increased with increasing concentration (Figure S2). In the fluorescence spectra of compounds in different solvents, fluorescent intensity of **X1**−**X3** was enhanced dramatically in low polar solvent compared to that in H_2O (Figure S3). Moreover, fluorescent intensity of **N1**−**N3** in different solvents caused a great difference. These results indicated that the fluorescence changed when probes bound to GPR120.

Pharmacologic Properties. In cytotoxicity assay, the CCK-8 assay was used to measure the cytotoxicity of probes in HEK-293 cells and PC-3 cells. Subsequently, HEK-293 cells and PC-3 cells would be applied in follow-up experiments. As is shown in Table 1, IC_{50} of each probe was at least 51.7 ± 4.8 μM after 24 h incubation, which indicated that each probe represented acceptable cytotoxicity in two cell lines. Overall, the cytotoxicity of probes was negligible in follow-up assays because experiment duration was less than 3 h.

In biological activity assay, BRET-based β-arrestin-2 activity assay and calcium flux activity assay were conducted. The result is shown in Table 1. TUG-1197 exhibited pEC_{50} of 6.20 ± 0.20 in the β-arrestin-2 assay and 6.10 ± 0.27 in the Ca^{2+} assay. There was no significant decrease in the activity of the probe compared to that of TUG-1197. The results of probes activity is basically the same between two assays. **N3** and **X1** stood out as the most potent GPR120 fluorescent agonists in respective series.

In target selection experiment, because carboxylic agonists responded to GPR40, the activity of probes on GPR40 was used to reflect the selectivity of GPR120. The substances in the experiment proved to have little effect on the result (Figure S4). The result is shown in Figure 1, **N3** and **X1** showed little fluorescent signal compared to L6. The result showed that sulfonamide probes had higher selectivity on GPR120 over carboxylic compounds.

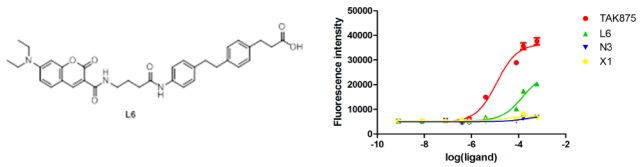

Figure 1. Ca^{2+} response by compounds L6, **N3**, **X1**, and TAK875 in CHO cells expressing GPR40 transiently.

Fluorescence Imaging and Monitoring. In cell-imaging experiments, studies were conducted using living cells. HEK293 cells were designed as a positive group and GPR120 was distributed on cell membrane, while PC-3 cells were a negative group. The cell-imaging result (Figure 2, Figures S5 and S6) showed that, after the addition of probes, fluorescence was observed on the membrane of HEK293 cells. In PC-3 cells, there was no fluorescence observed. Cell imaging proved preliminarily that probes can localize GPR120 expressed on HEK293 cells. In monitoring internalization assay, fluorescence was expanded from cell membrane to cytoplasm over time and fluorescence intensity increased gradually after addition of **N3** (or **X1**). The result proved that GPR120 entered cells after agonist activation. It showed that probes could be utilized in GPR120 biological mechanisms by real-time monitoring. Nevertheless, the experiment could not maintain the environment at 37 °C, 5% CO_2; the state of the cells deteriorated gradually (Figures S7 and S8).

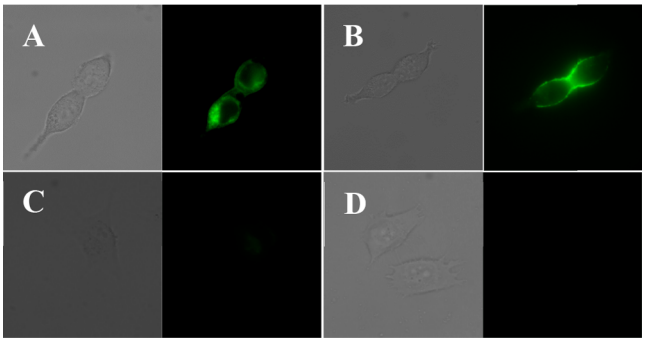

Figure 2. Exposure time kept pace with 300 ms. The fluorescent imaging was performed and processed in the GFP channel, objective lens, 63×, in Zeiss Axio Observer A1. (A) Imaging result of **N3** (200 nM) in HEK293 cells. (B) Imaging result of **X1** (200 nM) in PC-3 cells. (C) Imaging result of **N3** (200 nM) in PC-3 cells. (D) Imaging result of **X1** (200 nM) in PC-3 cells.

BRET Assay Based on Probes. For BRET assay, GPR120 was transfected with Renilla luciferase (Rluc) expressing in HEK293 cell. Rluc, a bioluminescent enzyme, can oxidize its substrates and exhibit fluorescence. Moreover, DeepBlue C was selected as the substrate of Rluc. Therefore, when probes bound to GPR120-Rluc, energy transfer occurred between Rluc and the probe at 420 nm after addition of DeepBlue C (Figure 4).

In saturation BRET binding experiments, after **N3** (or **X1**) bound to cell membrane to saturation, BRET value increased as the concentration of probes increased because of nonspecific binding (Figure 3). The saturation assay was conducted to obtain K_D = 10.17 ± 3.01 nM for **N3** and K_D = 10.04 ± 3.76

DOI: 10.1021/acs.analchem.9b04157
Anal. Chem. 2019, 91, 15235−15239

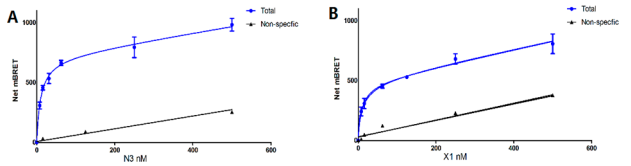

Figure 3. Saturation binding experiment of **N3** (**X1**) while nonspecific binding is measured by 10 μM TUG-1197. (A) Representative saturation binding experiment of **N3**. (B) Representative saturation binding experiment of **X1**.

nM for **X1**. By modeling of the computation using Graphpad Prism 5, effect of nonspecific binding could be ignored when the concentration of **N3** was less than 90.5 nM and **X1** was less than 82.6 nM.

In kinetic BRET binding experiments, the off and on rates were established to be k_{on} = 8.73 × 10^7 ± 3.26 × 10^7 min^{-1} M^{-1}, k_{off} = 0.141 ± 0.0109 min^{-1} for N3 and k_{on} = 8.14 × 10^7 ± 5.12 × 10^7 min^{-1} M^{-1}, k_{off} = 0.431 ± 0.0442 min^{-1} for **X1**. The k_{off} and k_{on} values yielded a K_d value of 1.6 nM for **N3** and 5.3 nM for X1 (Figure 4).

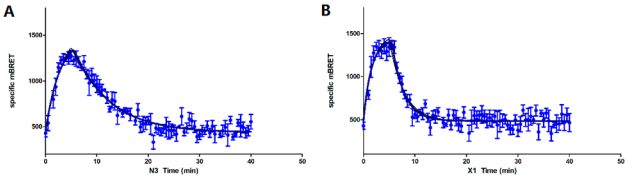

Figure 4. Kinetic binding experiments of **N3** (**X1**); 5 min after the addition of the fluorescent probes (50 nM), TUG-1197 (5 μM) was added to make the probe dissolve from GPR120. (A) Representative kinetic binding experiment of **N3**. (B) Representative kinetic binding experiment of **X1**.

In displacement BRET binding assay, we chose some representative compounds. TUG-891 was a carboxylic GPR120 agonist, GSK137647A and TUG-1197 were sulfonamide GPR120 agonists, AH-7614 was a sulfonamide GPR120 antagonist, and GW9508 was a carboxylic GPR40 agonist. Compounds could reduce BRET value by a competition binding assay in the presence of probes. As is shown in Table 2, the obtained K_i value was exhibited, which was similar to the

Table 2. Comparison of Results in BRET Assay to Reference Data

	BRET binding assay pK_i		
method compd	N3	X1	Ca^{2+} pEC^{50} [a]
TUG-891	7.18 ± 0.21	7.10 ± 0.07	7.02 ± 0.09
TUG-1197	6.48 ± 0.23	6.29 ± 0.49	6.63 ± 0.13
GSK137647A	6.56 ± 0.18	5.98 ± 0.18	6.30 ± 0.20
GW9508	5.83 ± 0.26	6.11 ± 0.09	5.46 ± 0.09
AH-7614	~3.57	~4.24	<4.5

[a] Ca^{2+} pEC_{50} values are reported in the literature.[13,14,24]

theoretical activity value acquired by calcium flux activity assay (response curves in Figures S9 and S10). The result showed that this displacement BRET binding assay could be used as a high-throughput screening method of GPR120 chemical library.

CONCLUSION

In this study, we designed and synthesized six small-molecule sulfonamide fluorescent probes for GPR120, which exhibited high selectivity for GPR120. These probes possessed good optical properties and low cytotoxicity and had high biological activity for GPR120. The probes could be used in localization and visualization of GPR120 in living cells. With the BRET-based binding assay, we could know the thermodynamic and kinetic parameters of probes **N3** and **X1**. Moreover, the BRET-based binding assay with molecules **N3** and **X1** for high-throughput screening had been established successfully to seek various agonists and antagonists of GPR120. It is expected that these probes can be used in further research for molecular pharmacology and drug discovery of GPR120.

ASSOCIATED CONTENT

Supporting Information

The Supporting Information is available free of charge on the ACS Publications website at DOI: 10.1021/acs.analchem.9b04157.

Full synthetic procedure, excitation and emission spectra of probes, selectivity test, fluorescence imaging results, competition curves, and NMR, MS, HRMS, and HPLC spectra (PDF)

AUTHOR INFORMATION

Corresponding Author

*Tel./Fax: +86-531-8838-2006. E-mail: dulupei@sdu.edu.cn (L.D.).

ORCID

Minyong Li: 0000-0003-3276-4921

Lupei Du: 0000-0003-0531-8985

Author Contributions

#P.L. and S.M. contributed equally to this work. The manuscript was written through contributions of all authors.

Notes

The authors declare no competing financial interest.

ACKNOWLEDGMENTS

The present work was supported by grants from the National Natural Science Foundation of China (No. 81874308) and the Key Research and Development Project of Shandong Province (No. 2018GSF118211).

REFERENCES

(1) Christiansen, E.; Watterson, K. R.; Stocker, C. J.; Sokol, E.; Jenkins, L.; Simon, K.; Grundmann, M.; Petersen, R. K.; Wargent, E. T.; Hudson, B. D.; Kostenis, E.; Ejsing, C. S.; Cawthorne, M. A.; Milligan, G.; Ulven, T. *Br. J. Nutr.* **2015**, *113* (11), 1677−88.

(2) Hirasawa, A.; Tsumaya, K.; Awaji, T.; Katsuma, S.; Adachi, T.; Yamada, M.; Sugimoto, Y.; Miyazaki, S.; Tsujimoto, G. *Nat. Med.* **2005**, *11* (1), 90−4.

(3) Oh, D. Y.; Talukdar, S.; Bae, E. J.; Imamura, T.; Morinaga, H.; Fan, W.; Li, P.; Lu, W. J.; Watkins, S. M.; Olefsky, J. M. *Cell* **2010**, *142* (5), 687−98.

(4) Iwasaki, K.; Harada, N.; Sasaki, K.; Yamane, S.; Iida, K.; Suzuki, K.; Hamasaki, A.; Nasteska, D.; Shibue, K.; Joo, E.; Harada, T.; Hashimoto, T.; Asakawa, Y.; Hirasawa, A.; Inagaki, N. *Endocrinology* **2015**, *156* (3), 837−46.

(5) Miyauchi, S.; Hirasawa, A.; Iga, T.; Liu, N.; Itsubo, C.; Sadakane, K.; Hara, T.; Tsujimoto, G. *Naunyn-Schmiedeberg's Arch. Pharmacol.* **2009**, *379* (4), 427−34.

DOI: 10.1021/acs.analchem.9b04157
Anal. Chem. 2019, 91, 15235−15239

(6) Zhang, D.; So, W. Y.; Wang, Y.; Wu, S. Y.; Cheng, Q.; Leung, P. S. *Clin. Sci.* **2017**, *131* (3), 247−260.
(7) Zhang, D.; Leung, P. S. *Drug Des., Dev. Ther.* **2014**, *8*, 1013−27.
(8) Tanaka, T.; Katsuma, S.; Adachi, T.; Koshimizu, T. A.; Hirasawa, A.; Tsujimoto, G. *Naunyn-Schmiedeberg's Arch. Pharmacol.* **2008**, *377* (4−6), 523−7.
(9) Tanaka, T.; Yano, T.; Adachi, T.; Koshimizu, T. A.; Hirasawa, A.; Tsujimoto, G. *Naunyn-Schmiedeberg's Arch. Pharmacol.* **2008**, *377* (4−6), 515−22.
(10) Oh, D. Y.; Walenta, E.; Akiyama, T. E.; Lagakos, W. S.; Lackey, D.; Pessentheiner, A. R.; Sasik, R.; Hah, N.; Chi, T. J.; Cox, J. M.; Powels, M. A.; Di Salvo, J.; Sinz, C.; Watkins, S. M.; Armando, A. M.; Chung, H.; Evans, R. M.; Quehenberger, O.; McNelis, J.; Bogner-Strauss, J. G.; Olefsky, J. M. *Nat. Med.* **2014**, *20* (8), 942−7.
(11) Liu, J.; Tian, C.; Jiang, T.; Gao, Y.; Zhou, Y.; Li, M.; Du, L. *ACS Med. Chem. Lett.* **2017**, *8* (4), 428−432.
(12) Li, A.; Li, Y.; Du, L. *Future Med. Chem.* **2015**, *7* (11), 1457−68.
(13) Azevedo, C. M.; Watterson, K. R.; Wargent, E. T.; Hansen, S. V.; Hudson, B. D.; Kepczynska, M. A.; Dunlop, J.; Shimpukade, B.; Christiansen, E.; Milligan, G.; Stocker, C. J.; Ulven, T. *J. Med. Chem.* **2016**, *59* (19), 8868−8878.
(14) Sparks, S. M.; Chen, G.; Collins, J. L.; Danger, D.; Dock, S. T.; Jayawickreme, C.; Jenkinson, S.; Laudeman, C.; Leesnitzer, M. A.; Liang, X.; Maloney, P.; McCoy, D. C.; Moncol, D.; Rash, V.; Rimele, T.; Vulimiri, P.; Way, J. M.; Ross, S. *Bioorg. Med. Chem. Lett.* **2014**, *24* (14), 3100−3.
(15) Nayab, P. S.; Pulaganti, M.; Chitta, S. K.; Abid, M.; Uddin, R. *J. Fluoresc.* **2015**, *25* (6), 1905−20.
(16) Liu, Z.; Jiang, T.; Wang, B.; Ke, B.; Zhou, Y.; Du, L.; Li, M. *Anal. Chem.* **2016**, *88* (3), 1511−5.
(17) Wagner, B. D. *Molecules* **2009**, *14* (1), 210−37.
(18) Jung, Y.; Jung, J.; Huh, Y.; Kim, D. *J. Anal. Methods Chem.* **2018**, *2018*, 5249765.
(19) Stoddart, L. A.; Johnstone, E. K. M.; Wheal, A. J.; Goulding, J.; Robers, M. B.; Machleidt, T.; Wood, K. V.; Hill, S. J.; Pfleger, K. D. G. *Nat. Methods* **2015**, *12* (7), 661−663.
(20) Nishihara, R.; Suzuki, H.; Hoshino, E.; Suganuma, S.; Sato, M.; Saitoh, T.; Nishiyama, S.; Iwasawa, N.; Citterio, D.; Suzuki, K. *Chem. Commun. (Cambridge, U. K.)* **2015**, *51* (2), 391−4.
(21) Jenkins, L.; Brea, J.; Smith, N. J.; Hudson, B. D.; Reilly, G.; Bryant, N. J.; Castro, M.; Loza, M. I.; Milligan, G. *Biochem. J.* **2010**, *432* (3), 451−9.
(22) Christiansen, E.; Hansen, S. V.; Urban, C.; Hudson, B. D.; Wargent, E. T.; Grundmann, M.; Jenkins, L.; Zaibi, M.; Stocker, C. J.; Ullrich, S.; Kostenis, E.; Kassack, M. U.; Milligan, G.; Cawthorne, M. A.; Ulven, T. *ACS Med. Chem. Lett.* **2013**, *4* (5), 441−445.
(23) Srivastava, A.; Yano, J.; Hirozane, Y.; Kefala, G.; Gruswitz, F.; Snell, G.; Lane, W.; Ivetac, A.; Aertgeerts, K.; Nguyen, J.; Jennings, A.; Okada, K. *Nature* **2014**, *513* (7516), 124−7.
(24) Moniri, N. H. *Biochem. Pharmacol.* **2016**, *110*−*111*, 1−15.

DOI: 10.1021/acs.analchem.9b04157
Anal. Chem. 2019, 91, 15235−15239